

PySAP: Python Sparse Data Analysis Package for Multidisciplinary Image Processing

S. Farrens^{a,b}, A. Grigis^b, L. El Gueddari^b, Z. Ramzi^{a,b}, Chaithya G. R.^b, S. Starck^c, B. Sarthou^d, H. Cherkaoui^b, P. Ciuciu^b, J.-L. Starck^a

^aAIM, CEA, CNRS, Université Paris-Saclay, Université Paris Diderot, Sorbonne Paris Cité, F-91191 Gif-sur-Yvette, France

^bCEA/DRF/Joliot NeuroSpin, Université Paris-Saclay, F-91191 Gif-sur-Yvette, France

^cEPITA, 14-16 rue Voltaire, 94270 Le Kremlin-Bicêtre, France

^dENSTA ParisTech, 828 Boulevard des Maréchaux, 91120 Palaiseau, France

Abstract

We present the open-source image processing software package PySAP (Python Sparse data Analysis Package) developed for the COmpressed Sensing for Magnetic resonance Imaging and Cosmology (COSMIC) project. This package provides a set of flexible tools that can be applied to a variety of compressed sensing and image reconstruction problems in various research domains. In particular, PySAP offers fast wavelet transforms and a range of integrated optimisation algorithms. In this paper we present the features available in PySAP and provide practical demonstrations on astrophysical and magnetic resonance imaging data.

Keywords: Image processing, convex optimisation, reconstruction, open-source software

1. Introduction

The ability to obtain high quality data in a short amount of time or indeed to recover high resolution images from undersampled blurred and noisy data can significantly improve the results of experiments potentially leading to new and exciting scientific discoveries. While the benefits of the mathematical methods that make this possible are relatively well known, robust and easy-to-use software tools that implement these techniques are extremely rare. The Compressed Sensing for Magnetic Resonance Imaging and Cosmology (COSMIC) project (<http://cosmic.cosmostat.org/>) was funded by the Fundamental Research Division (DRF) at the French Alternative Energies and Atomic Energy Commission (CEA) to provide precisely these tools.

COSMIC is a collaboration between two CEA groups with signal processing expertise: NeuroSpin, specialists in Magnetic Resonance Imaging (MRI), and CosmoStat, specialists in astrophysical image analysis. There is significant overlap in these fields, especially for astrophysical radio imaging that, like MRI, collects data in Fourier space. The primary output of this collaboration has been the development of the Python Sparse data Analysis Package (PySAP).

PySAP is an open-source software package written in Python that provides highly optimised sparse image transforms and a library of modular optimisation tools for solving linear inverse problems. While PySAP has been designed with specific applications to the MRI and astrophysics domains in mind, the versatility of the software and the universality of the mathematical techniques mean

that it can also be applied to a variety of other imaging domains such as microscopy, tomography and echography.

Compared to existing inverse problem solving packages, such as SPAMS (Mairal et al., 2009b,a, 2010; Jenatton et al., 2010) and SigPy (Ong and Lustig, 2019), PySAP offers efficient implementations of specialised multiscale transforms. In particular, PySAP provides undecimated wavelet transforms, which are well suited to astrophysical images, and 3D wavelet transforms, which are of particular interest for MR image processing (see Sec. 2.1). PySAP also includes several detailed applications of these tools to data to facilitate user understanding (see Sec. 3).

This paper is organised as follows. Section 2 provides a detailed description of the structure and features of PySAP with particular focus on the image transforms and optimisation tools. Section 3 demonstrates practical applications of PySAP on MRI and astrophysical data. Finally, conclusions and plans for the future development of the package are presented.

2. PySAP Features

In essence, the base PySAP package serves as a front-end that comprises several specialised modules. PySAP provides a simplified framework in which to combine these modules as well as managing file IO, visualisation and exception handling.

The core modules that provide the PySAP features are:

- Sparse2D: Sparse Image Transforms
- ModOpt: Modular Optimisation Tools

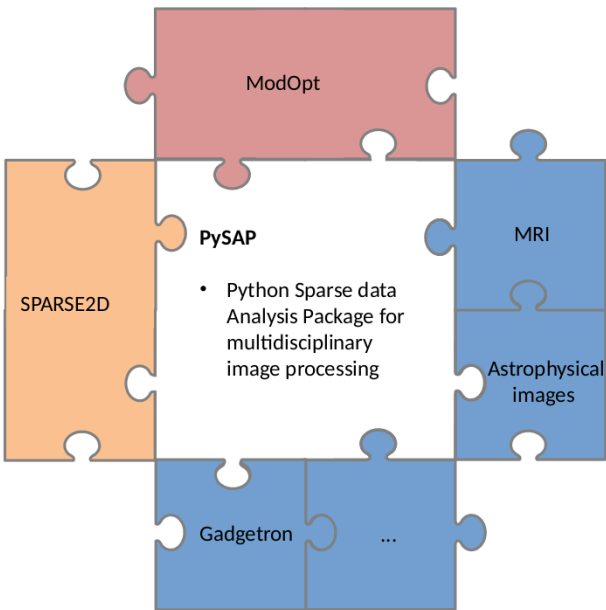


Figure 1: Illustration of the structure of the PySAP package. The SPARSE2D and ModOpt core libraries are represented in orange and red, respectively. The various plug-in applications appear in blue.

- Plug-ins

Fig. 1 illustrates the core structure of the PySAP package. Each of these modules is described in detail in the following subsections.

2.1. Sparse Image Transforms

The most essential tools for implementing compressed sensing or sparsity in signal processing problems are efficient dictionaries well suited to the data at hand. In practice, these dictionaries correspond to a series of data transforms ranging from wavelets to curvelets that can convert the data into a domain where the majority of the information is concentrated in very few non-zero coefficients, a concept called sparsity or compressibility.

Sparse2D is a C++ package, which forms part of iSAP (Interactive Sparse Astronomical data Analysis Packages), that provides a wide range of robust and efficient sparse transforms for 1D, 2D and 3D signals. In particular, the package includes a collection of undecimated wavelet transforms (UWT) that provide shift invariant properties for image reconstruction, such as the starlet transform (Starck et al., 2007) or the 7/9 UWT. These transforms are well documented in Starck et al. (2015). Sparse2D also includes 2D1D and curvelets transforms, enabling the sparse decomposition of various types of data. A full list of the available transforms is provided in the Appendix A. These software tools have been extensively tested on astrophysical data producing high quality results on a range of different topics (Bobin et al., 2014; Leonard et al., 2014; Ngolè Mboula et al., 2015; Lanusse et al., 2016). The fact that this package relies on a set of fixed multiscale dictionaries

means that the transforms are very computationally efficient and are therefore ideally suited to on-line MR image reconstruction (El Gueddari et al., 2019a).

PySAP provides Python bindings for the Sparse2D C++ libraries, thus enabling fast and efficient implementation of the sparse transforms inside of a Python environment. This allows these tools to be more easily integrated into optimisation problems without any loss of performance (see section 2.2). Additionally, through the PySAP interface, Sparse2D transforms can be applied to MRI data separately on the real and imaginary parts.

In addition to Sparse2D, PySAP also includes all of the transforms provided in PyWavelets (Lee et al., 2019).

2.2. Modular Optimisation Tools

Linear inverse problems, such as compressed sensing, are ill-posed because they are under-determined, *i.e.* the number of measurements is far below the number of image pixels. To cope with this issue and make the inverse problem well posed, one usually resorts to regularisation. The image solution is then obtained as the minimiser of an optimisation problem. One of the main features of PySAP is a series of modular optimisation tools designed for solving linear inverse problems that comprise a subpackage called ModOpt.

This package is particularly well suited for solving linear inverse imaging problems of the following form

$$\mathbf{y} = \mathbf{H}\mathbf{x} + \mathbf{n} \quad (1)$$

where \mathbf{y} is the observed image obtained from the detector in question, \mathbf{H} is a degradation matrix that could constitute blurring, sub-sampling, distortion, *etc.*, \mathbf{x} is the true image that one aims to recover and \mathbf{n} is noise.

ModOpt provides robust and extremely flexible implementations of cutting-edge optimisation algorithms such as Forward-Backward, FISTA (Beck and Teboulle, 2009), Generalised Forward-Backward (Raguet et al., 2013), Condat-Vũ (Condat, 2013; Vũ, 2013) and POGM' (Kim and Fessler, 2018). For instance, these algorithms have been compared for MR image reconstruction in (Ramzi et al., 2019). The flexibility of these implementations is provided via means of Python class composition. All of the proximity and linear operators as well as the gradient utilised by a given algorithm can be provided as class instances that inherit a parent structure to ensure smooth cohesion. The modularity of this approach means that any potential bug can be easily identified and fixed, thus ensuring a well maintained and robust framework. Additionally, this structure facilitates the future implementation of virtually any optimisation algorithm.

Predefined proximity operators are provided for implementing sparse, low-rank and structurally sparse regularisation (*i.e.*, ℓ_1 , nuclear and mixed norms, respectively) as well as a positivity constraint, which is commonly required in image analysis problems. Tools are included that

allow the automatic setting of the regularisation parameters using the noise properties of the observed data. New proximity operator instances can easily be generated using the parent class. A list of the proximity operators currently available in ModOpt is provided in Table 1. This structure includes a method that automatically calculates a given operator’s contribution to the overall cost of the optimisation problem at hand.

The linear operator parent class enables the use of any of the sparse image transforms described in section 2.1, in fact this framework is flexible enough to allow the implementation of virtually any custom transform. The structure of this class also requires the definition of the adjoint process for a given transformation.

A standard gradient implementation of the form

$$\nabla F(\mathbf{x}) = \mathbf{H}^T(\mathbf{H}\mathbf{x} - \mathbf{y}) \quad (2)$$

is included, where $F(\mathbf{x})$ is a convex function of the form $F(\mathbf{x}) = \frac{1}{2}\|\mathbf{H}\mathbf{x} - \mathbf{y}\|_2^2$. The parent class structure ensures that the gradient required for a given inverse problem can be easily implemented. As with the proximity operators, the gradient’s contribution to the total cost is built into the class structure.

A cost function class is also provided that automatically sums up the contributions from the proximity and gradient operators. This class has a built-in framework to test for convergence up to a given tolerance.

Finally, a reweighting class is provided to counteract the bias introduced into a given solution owing to the use of soft-thresholding in sparse regularisation. At present, the method of Candès et al. (2008) is included.

The combination of these tools enables the user to very quickly prototype robust codes for tackling a variety of inverse imaging problems.

2.3. Plug-ins

PySAP also provides application specific plug-ins. In this module algorithms and operators from ModOpt can be combined with Sparse2D transforms to develop tools for a given application. The objective being to produce user-friendly functions, designed to solve well defined problems, that can be applied directly to data.

At present, this module contains plug-ins that demonstrate the applicability of PySAP to astrophysical and MRI data (`pysap-astro` and `pysap-mri`, respectively). For example, the MRI plug-in `pysap-mri` (El Gueddari et al., 2020) adds the ability to deal with non-Cartesian data using non-uniform or non-equispaced FFT tools, while the astrophysics plug-in provides easy-to-use tools for denoising or deconvolving survey images. A specific plug-in, called `pysap-data` hosts the data sets used in the examples provided, while another one, called `pysap-tutorial`, contains materials for hands-on sessions. In the near future, two supplementary plug-ins will be released for other imaging techniques such as electron tomography (`pysap-comset`) (Lin et al., 2020), and electron microscopy (`pysap-emicro`).

The plug-in framework has been designed to promote collaboration by providing a template for creating new plug-ins for virtually any imaging domain.

3. Practical Applications

3.1. Astrophysical Images

One straightforward application of PySAP on astrophysical data is to the problem of galaxy image deconvolution. Astrophysical images obtained with optical telescopes are subject to a blurring caused by internal factors, such as imperfections in the optical system, and external factors, such as the atmosphere for ground based instruments. The sum of these aberrations is commonly referred to as the Point Spread Function (PSF).

Removing the effects of the PSF from noisy observations amounts to solving a non-trivial inverse problem that requires the use of regularisation owing to the ill-conditioned nature of the degradation matrix, which corresponds to convolution with the PSF in this case. This problem can be solved using sparse regularisation following the same prescription described in Farrens et al. (2017) using PySAP. A deconvolution example is provided in PySAP that demonstrates this process in a few lines of code. This example takes a COSMOS (Koekemoer et al., 2007; Scoville et al., 2007b,a) galaxy image that has been processed to remove noise (see Farrens et al., 2017) as the true image that one aims to recover. An observation is then simulated by convolving this image with an anisotropic PSF and adding white Gaussian noise. This example performs deconvolution using the Condat–Vũ algorithm. An isotropic undecimated wavelet transform from Sparse2D is used for the linear operator, and a positivity constraint and soft-thresholding of the sparse coefficients are used as the proximity operators. The results of this example are shown in Figure 2.

Another application is simply removing noise from observations. This is a particularly challenging problem when the object in question contains important high-frequency spatial features that need to be preserved. Figure 3 presents the results of denoising an image of the galaxy NGC2997 using PySAP. For this example white Gaussian noise is added to the clean image and then the same isotropic undecimated wavelet transform from Sparse2D is used to decompose the noisy image, which is in turn thresholded by weights learned from the noisy image itself.

Note that the data used for the examples presented in this paper are provided in PySAP (in the `pysap-data` plug-in). Therefore, all of the example outputs can be reproduced exactly by users.

3.2. MRI

MRI is probably one of the most successful applications of compressed sensing. The ability to reconstruct high-fidelity MR images from massively undersampled data in a short amount of time is of paramount importance. This

Table 1: List of proximity operators currently available in ModOpt. The k -support norm generalises the group-LASSO $\ell_{2,1}$ norm (Yuan and Lin, 2006) for imposing structured sparsity with overlapping groups, typically in the context of calibrationless MR image reconstruction. A particular case of Ordered Weighted L1 norm (OWL) that implements structured sparsity is OSCAR regularisation (Bondell and Reich, 2008; El Gueddari et al., 2019b).

Proximity Operator	Application
Positivity	Image analysis
ℓ_1 Minimisation	Sparse regularisation
ℓ_* Minimisation	Low-rank regularisation
ℓ_2 Minimisation	Ridge regularisation
$\alpha\ell_1 + \beta\ell_2$ Minimisation ($\alpha, \beta \geq 0$)	Elastic-net regularisation
Ordered weighted ℓ_1 norm (Zeng and Figueiredo, 2014)	ℓ_∞ -based Structured sparsity regularisation
k -support norm (Argyriou et al., 2012)	ℓ_2 -based Structured sparsity regularisation

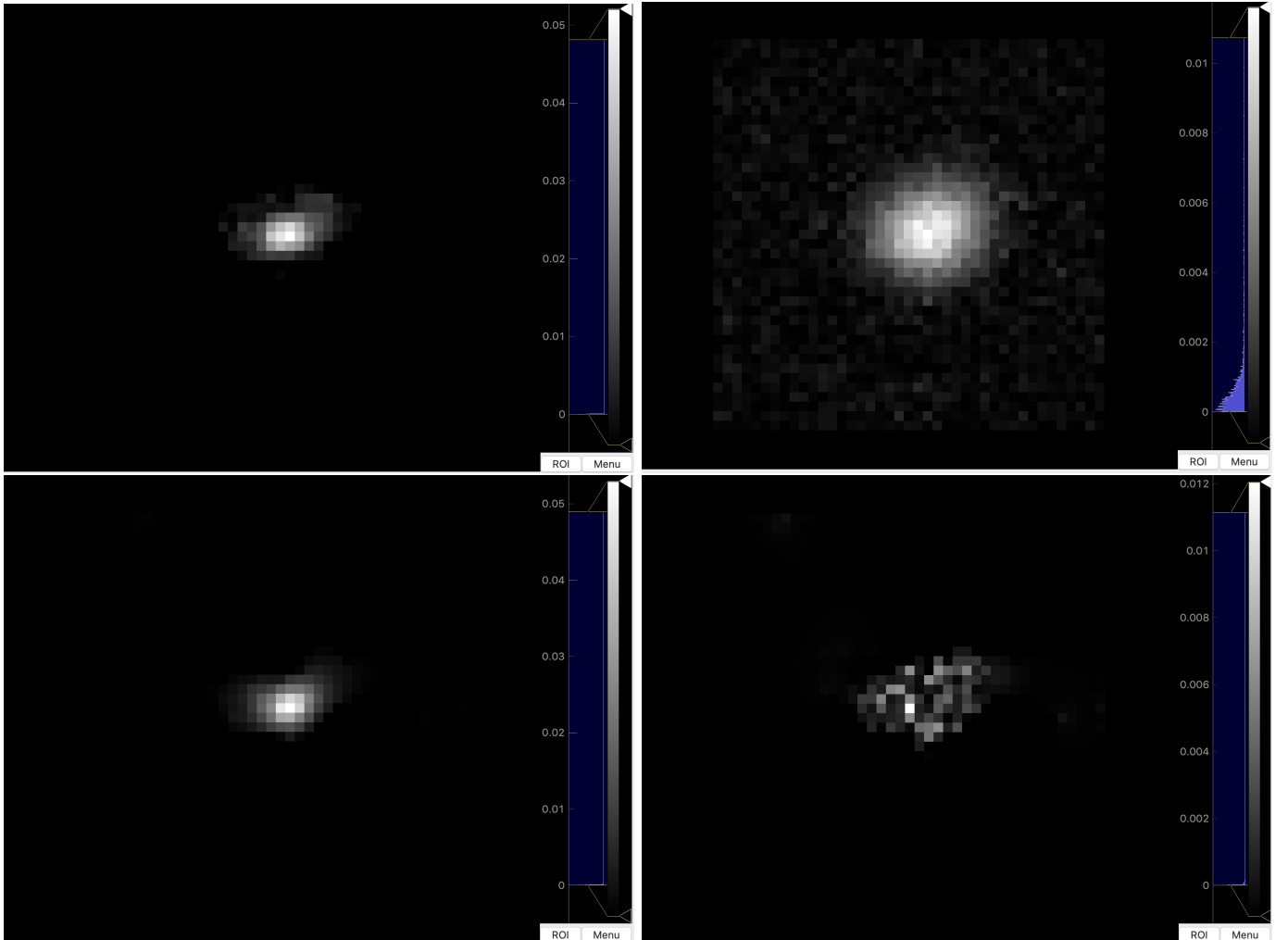


Figure 2: Example of galaxy image deconvolution using PySAP. *Top left*: True galaxy image, *Top right*: observed galaxy image, *Bottom left*: deconvolved galaxy image, *Bottom right*: deconvolution residual.

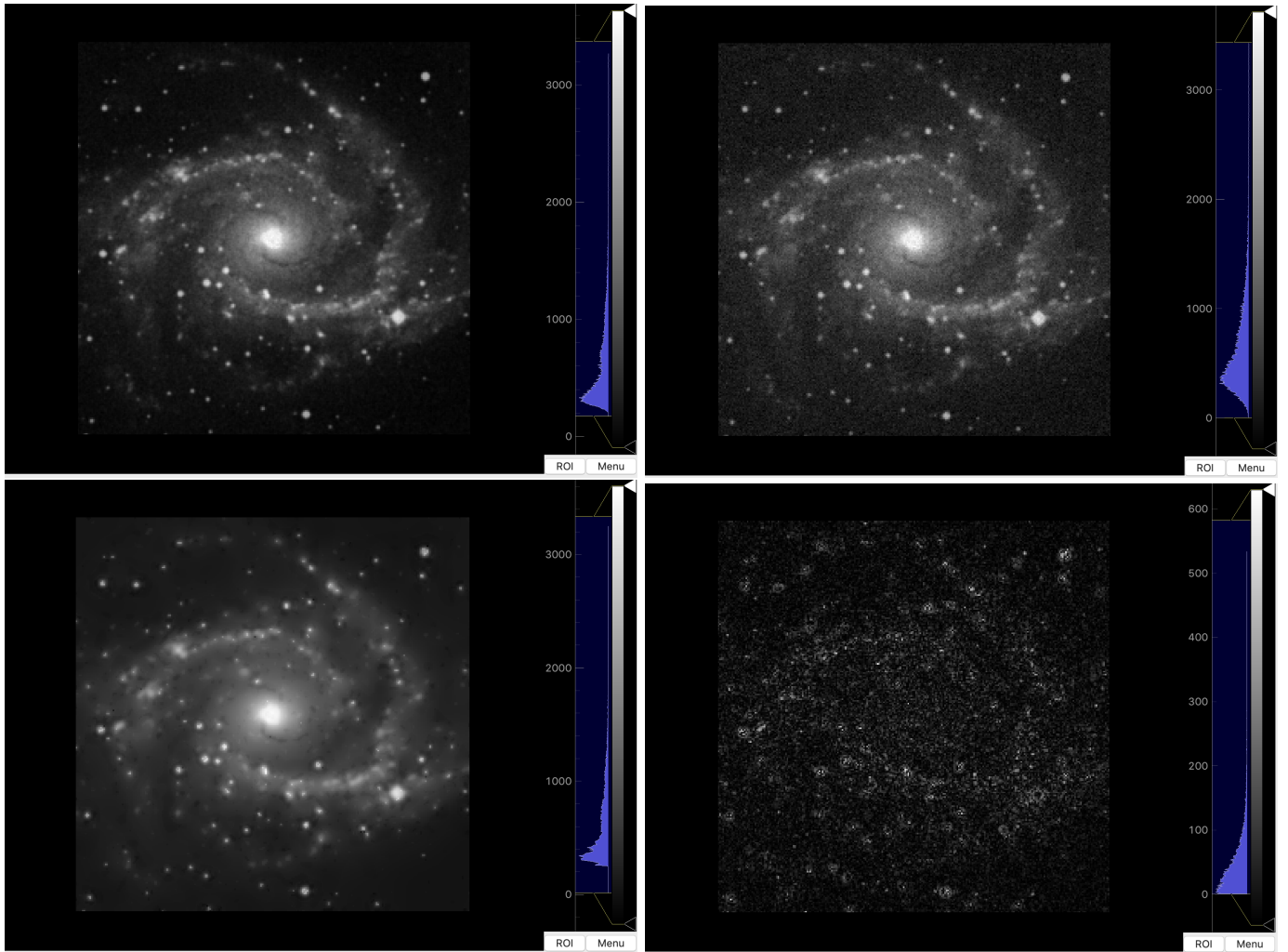


Figure 3: Example of galaxy image denoising using PySAP. *Top left:* True galaxy image, *Top right:* observed galaxy image, *Bottom left:* denoised galaxy image, *Bottom right:* denoising residual.

is achievable as the data collected in the Fourier domain (called k-space in MRI) may be acquired using variable density sampling (VDS) along a small number of trajectories (or shots), either Cartesian or not (*e.g.* radial Jackson et al. (1992), spiral Meyer et al. (1992) or more custom like Sparkling Lazarus et al. (2017, 2019)). The images can then be reconstructed using state-of-the-art optimisation algorithms. The idea is to take advantage of these time-saving strategies, not only to increase spatial resolution in anatomical imaging, but also to reduce sensitivity to motion. Importantly, PySAP is able to deal with both single and multi-channel 2D and 3D k-space data using GPU versions of NFFT operators. 3D VDS may be particularly relevant to improve the spatio-temporal resolution in functional MRI.

Take, for example, the problem of compressed sensing parallel imaging reconstruction. For this example let L be the number of coils used to acquire the NMR signal, n the image dimension and $N = n \times n$ be the number of pixels of a 2D complex-valued image $\mathbf{x} \in \mathbb{C}^N$ to be reconstructed and M the number of samples collected per channel during acquisition. We denote by $\mathbf{y}_\ell \in \mathbb{C}^M$ the complex-valued data recorded by the ℓ^{th} channel, $\mathbf{S}_\ell \in \mathbb{C}^{N \times N}$ the corresponding diagonal sensitivity matrix. This matrix \mathbf{S}_ℓ reflects how well the ℓ th receiver coil captures part of the object \mathbf{x} . Let F be the Fourier transform and $\Omega \subset \{1, \dots, N\}$ the sampling pattern in the k -space, with $|\Omega| = M \ll N$. The CS-PI acquisition model thus reads:

$$\mathbf{y}_\ell = \mathcal{F}_\Omega \mathbf{S}_\ell \mathbf{x} + \mathbf{n}_\ell, \quad \forall \ell = 1 : L, \quad (3)$$

where \mathbf{n}_ℓ is additive zero-mean Gaussian noise of variance σ_ℓ^2 , which can be characterised by a separate scan (without RF pulse) considering the same bandwidth as the prospective CS acquisition. In the case of Cartesian undersampling, $\mathcal{F}_\Omega = \mathbf{\Omega} \mathbf{F}$ where $\mathbf{\Omega}$ is a binary sampling mask with M non-zero entries and \mathbf{F} is the fast Fourier transform (FFT). In the case of non-Cartesian undersampling, \mathcal{F}_Ω is the Non-equispaced Fourier transform (NFFT). In the case where one assumes the sensitivity matrices $(\mathbf{S}_\ell)_{\ell=1}^L$ are known in advance, this problem can easily be solved using sparse regularisation following the same prescription described in Chaari et al. (2011); Guerquin-Kern et al. (2011) using PySAP in just a few lines of code. In the context of VDS, one may extract low frequency information from k-space data $(\mathbf{y}_\ell)_{\ell=1}^L$ to estimate the sensitivity maps $(\mathbf{S}_\ell)_{\ell=1}^L$ prior to reconstruction: this is called self-calibrated MR image reconstruction and has been implemented in El Gueddari et al. (2018).

Several example applications to MR data are provided in the PySAP package. A first example is shown in Figure 4. It shows the reconstruction of an MR image from retrospectively undersampled k-space data. The original Cartesian data were collected in vivo on a healthy volunteer at 7 Tesla (Magnetom Siemens scanner, Erlangen, Germany) using a 32-channel (Nova Medical Inc., Washington, MA, USA) coil ($L = 32$) and a 2D T2*-weighted

GRE sequence (see details in (Lazarus et al., 2019)). To illustrate CS reconstruction algorithms, we actually used the reference image obtained as the square root of the sum of squares of 32 channels (see Fig. 4 top-left), which we retrospectively undersample. In that context, we emulated a single receiver coil to get rid of the estimation of sensitivity maps. Note however that specific algorithms are provided to extract these sensitivity matrices and perform image reconstruction in the dedicated plug-in for MRI as described in (El Gueddari et al., 2018, 2019b).

For educational purposes, we first used a Cartesian mask that implements variable density sampling along the phase encoding (vertical) direction. We kept only $N_c = 98$ phase encoding lines out of $n = 512$, leading to an undersampling factor $R = N/M$ equal to the acceleration factor in time $\text{AF} = n/N_c = 5.22$. The FISTA algorithm Beck and Teboulle (2009) was used for optimisation purposes with sparsity promoted with the decimated symmlet 8 transform. The image reconstructed in Figure 4 using this strategy outperforms the zero-filled inverse FFT by almost 0.1 in terms of structural similarity (SSIM) score (0.91 vs 0.82).

A second example is depicted in Figure 5, where retrospective radial undersampling was applied with only $N_c = 64$ shots out of $n = 512$ leading to a downsampling factor of $R = \text{AF} = 8$. The sparsity was promoted using an anisotropic undecimated wavelet transform from Sparse2D. The image reconstructed using this strategy outperforms the zero-filled inverse NFFT by 0.25 in terms of SSIM score (0.92 vs 0.67).

Note that as in these examples we only performed retrospective undersampling, $R = \text{AF}$, however, in prospective acceleration, one may gain in image quality using oversampling over each shot which leads to $R < \text{AF}$. Some codes spinets can be found in the PySAP documentation gallery:

https://python-pysap.readthedocs.io/en/latest/auto_gallery/gallery.html.

3.3. Gadgetron

Gadgetron natively supports Python packages and therefore PySAP can easily be installed on any MRI scanner where the Gadgetron framework is in place.

4. Conclusions

In this paper we have presented the image processing package PySAP, its principal features and example applications to MR and astrophysical images. In particular, examples demonstrate how PySAP can be applied to image processing problems such as denoising, deconvolution and compressed sensing employing state-of-the-art reconstruction algorithms and wavelet transforms. In each case the plug-in framework provides easy-to-use tools for solving these problems for specific applications.

The flexibility and modularity of this package permit a wide range of possible future developments. In particular,

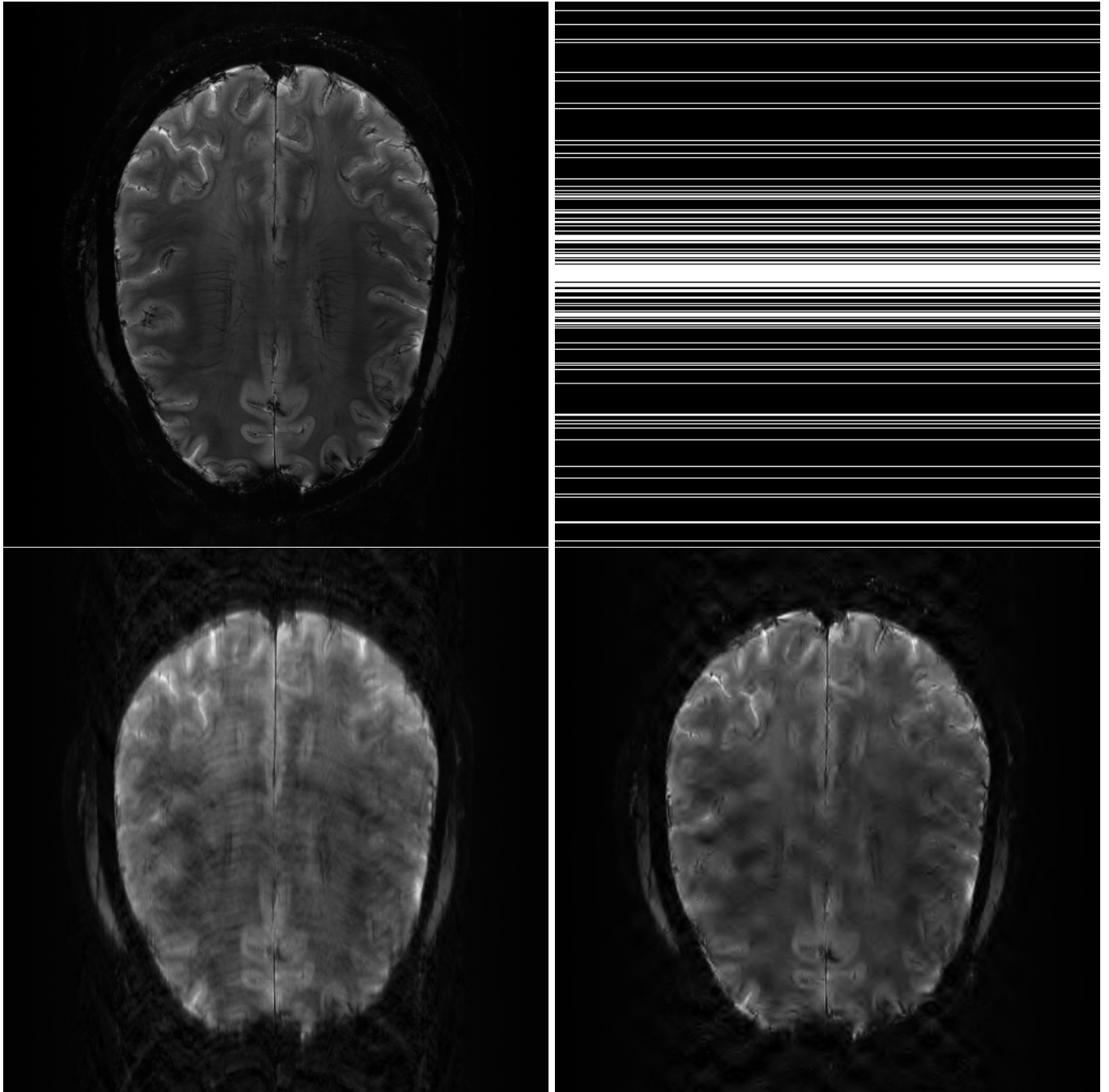


Figure 4: Cartesian MRI decimated wavelet-based reconstruction. *Top left:* Cartesian reference, *Top right:* K-space mask, *Bottom left:* Zero-filled reconstruction ($SSIM = 0.82$), *Bottom right:* Decimated wavelet based reconstruction ($SSIM = 0.91$).

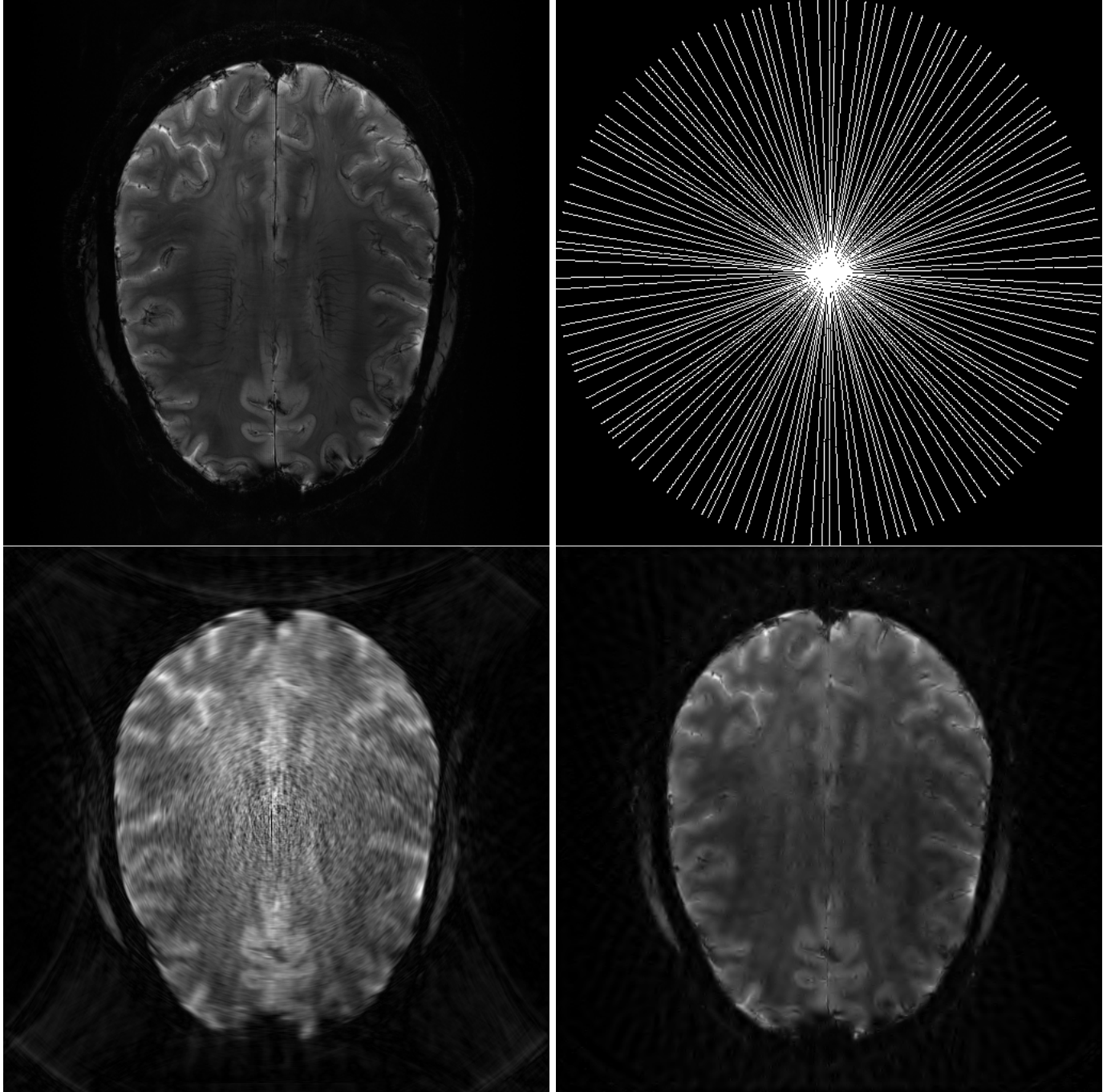


Figure 5: Non-cartesian MRI undecimated wavelet-based reconstruction. *Top left:* Cartesian reference, *Top right:* K-space mask, *Bottom left:* Zero-filled reconstruction ($SSIM = 0.67$), *Bottom right:* Undecimated wavelet based reconstruction ($SSIM = 0.92$).

we aim to continue to add new and cutting-edge optimisation algorithms, reweighting methods, *etc.* We additionally aim to add further features for handling 4D data and optimising the computation time by exploring GPU implementations. Another important aspect to which we plan to dedicate effort is to integrating machine and deep learning techniques into the existing architecture.

One of the most exciting uses of PySAP comes from the Gadgetron implementation. The universality of this system and the growing community mean that PySAP can readily be used at MRI scanners around the world, potentially leading to some fascinating developments in the biomedical imaging domain.

Finally, we intend to seek out new applications of this software in a variety of different fields. In fact, work has already begun on developing a PySAP plug-in for electron tomography and electron microscopy.

Reproducible research. In the spirit of reproducible research PySAP is made publicly available and fully open source. Documentation and installation instructions are available on the PySAP website (<https://python-pysap.readthedocs.io/>). The authors kindly request that any academic publications that make use of PySAP cite this paper.

Acknowledgments

The authors wish to acknowledge the COSMIC project funded by the CEA DRF-Impulsion call in 2016, the Cross-Disciplinary Program on Numerical Simulation (SILICOS-MIC project in 2018) of CEA, the French Alternative Energies and Atomic Energy Commission. They are also grateful to the UnivEarthS Labex program of Sorbonne Paris Cite (ANR-10-LABX-0023 and ANR-11- IDEX-0005-02), the European Community through the grant DEDALE (contract no. 665044) within the H2020 Framework Program of the European Commission, the Euclid Collaboration, the European Space Agency and the support of the Centre National d'Etudes Spatiales. The authors additionally acknowledge Hanaé Carrié and Fabrice Poupon for contributing to the development of this package.

References

Argyriou, A., Foygel, R., Srebro, N., 2012. Sparse Prediction with the k -Support Norm. pp. 1457–1465.

Beck, A., Teboulle, M., 2009. A fast iterative shrinkage-thresholding algorithm for linear inverse problems. *SIAM J. Img. Sci.* 2, 183–202. doi:10.1137/080716542.

Bobin, J., Sureau, F., Starck, J.L., Rassat, A., Paykari, P., 2014. Joint Planck and WMAP CMB map reconstruction. *Astronomy & Astrophysics* 563, A105. doi:10.1051/0004-6361/201322372.

Bondell, H.D., Reich, B.J., 2008. Simultaneous regression shrinkage, variable selection, and supervised clustering of predictors with OSCAR. *Biometrics* 64, 115–123. doi:10.1111/j.1541-0420.2007.00843.x.

Candès, E.J., Wakin, M.B., Boyd, S.P., 2008. Enhancing sparsity by reweighted l1 minimization. *J. Fourier Anal. Appl.* 14, 877–905. doi:10.1007/s00041-008-9045-x.

Chaari, L., Pesquet, J.C., Benazza-Benyahia, A., Ciuciu, P., 2011. A wavelet-based regularized reconstruction algorithm for SENSE parallelMRI with applications to neuroimaging. *Medical Image Analysis* 15, 185–201. doi:10.1016/j.media.2010.08.001.

Condat, L., 2013. A primal-dual splitting method for convex optimization involving Lipschitzian, proximable and linear composite terms. *J. Optim. Theory Appl.* 158, 460–479. doi:10.1007/s10957-012-0245-9.

El Gueddari, L., Chouzenoux, E., Pesquet, J.C., Ciuciu, P., 2019a. Online MR image reconstruction for Compressed Sensing acquisition in T_2^* imaging.

El Gueddari, L., Ciuciu, P., Chouzenoux, E., Vignaud, A., Pesquet, J.C., 2019b. Calibrationless OSCAR-based image reconstruction in compressed sensing parallel MRI. pp. 1532–1536.

El Gueddari, L., Giliyar Radhakrishna, C., Ramzi, Z., Farrens, S., Starck, S., Grigis, A., Starck, J.L., Ciuciu, P., 2020.

El Gueddari, L., Lazarus, C., Carrié, H., Vignaud, A., Ciuciu, P., 2018.

Farrens, S., Ngolè Mboula, F.M., Starck, J.L., 2017. Space variant deconvolution of galaxy survey images. *Astronomy & Astrophysics* 601, A66. doi:10.1051/0004-6361/201629709.

Guerquin-Kern, M., Haberlin, M., Pruessmann, K., Unser, M., 2011. A fast wavelet-based reconstruction method for magnetic resonance imaging. *IEEE Trans. Med. Imaging* 30, 1649–1660. doi:10.1109/TMI.2011.2140121.

Jackson, J.I., Nishimura, D.G., Macovski, A., 1992. Twisting radial lines with application to robust magnetic resonance imaging of irregular flow. *Magnetic Resonance in Medicine* 25, 128–139. doi:10.1002/mrm.1910250113.

Jenatton, R., Mairal, J., Obozinski, G., Bach, F., 2010.

Kim, D., Fessler, J.A., 2018. Adaptive Restart of the Optimized Gradient Method for Convex Optimization. doi:doi.org/10.1007/s10957-018-1287-4.

Koekemoer, A.M., Aussel, H., Calzetti, D., Capak, P., Giavalisco, M., Kneib, J.P., Leauthaud, A., Le Fèvre, O., McCracken, H.J., Massey, R., Mobasher, B., Rhodes, J., Scoville, N., Shopbell, P.L., 2007. The COSMOS Survey: Hubble Space Telescope Advanced Camera for Surveys Observations and Data Processing. *Astrophys. J. Suppl. Ser.* 172, 196–202. doi:10.1086/520086.

Lanusse, F., Starck, J.L., Leonard, A., Pires, S., 2016. High resolution weak lensing mass mapping combining shear and flexion. *Astronomy & Astrophysics* 591, A2. doi:10.1051/0004-6361/201628278.

Lazarus, C., Weiss, P., Chauffert, N., Mauconduit, F., Bottlaender, M., Vignaud, A., Ciuciu, P., 2017.

Lazarus, C., Weiss, P., Chauffert, N., Mauconduit, F., El Gueddari, L., Destrieux, C., Zemmoura, I., Vignaud, A., Ciuciu, P., 2019. SPARKLING: variable-density k-space filling curves for accelerated T_2^* -weighted MRI. *Magnetic Resonance in Medicine* 81, 3643–3661. doi:10.1002/mrm.27678.

Lee, G., Gommers, R., Waselewski, F., Wohlfahrt, K., Aaron, ., 2019. PyWavelets: A Python package for wavelet analysis. *J. Open Source Softw.* 4, 1237. doi:10.21105/joss.01237.

Leonard, A., Lanusse, F., Starck, J.L., 2014. GLIMPSE: accurate 3D weak lensing reconstructions using sparsity. *Monthly Notices of the Royal Astronomical Society* 440, 1281–1294. doi:10.1093/mnras/stu273.

Lin, J.M., Jacob, M., Saggi, Z., Ciuciu, P., Starck, J.L., 2020.

Mairal, J., Bach, F., Ponce, J., Sapiro, G., 2009a. Online dictionary learning for sparse coding. p. 87. doi:10.1145/1553374.1553463.

Mairal, J., Bach, F., Ponce, J., Sapiro, G., 2009b. Online learning for matrix factorization and sparse coding. *Journal of Machine Learning Research* 11. doi:10.1145/1756006.1756008.

Mairal, J., Jenatton, R., Obozinski, G., Bach, F., 2010. Network flow algorithms for structured sparsity. *Adv. Neural Inform. Process. Syst.* 23.

Meyer, C.H., Hu, B.S., Nishimura, D.G., Macovski, A., 1992. Fast spiral coronary artery imaging. *Magnetic Resonance in Medicine* 28, 202–213. doi:10.1002/mrm.1910280204.

Ngolè Mboula, F.M., Starck, J.L., Ronayette, S., Okumura, K., Amiaux, J., 2015. Super-resolution method using sparse regularization

for point-spread function recovery. *Astronomy & Astrophysics* 575, A86. doi:10.1051/0004-6361/201424167.

Ong, F., Lustig, M., 2019.

Raguet, H., Fadili, J., Peyré, G., 2013. A generalized forward-backward splitting. *SIAM Journal on Imaging Sciences* 6, 1199–1226. doi:10.1137/120872802, arXiv:1108.4404.

Ramzi, Z., Ciuciu, P., Starck, J.L., 2019. Benchmarking proximal methods acceleration enhancements for CS-acquired MR image analysis reconstruction. URL: <https://hal.inria.fr/hal-02298569>.

Scoville, N., Abraham, R.G., Aussel, H., Barnes, J.E., Benson, A., Blain, A.W., Calzetti, D., Comastri, A., Capak, P., Carilli, C., Carlstrom, J.E., Carollo, C.M., Colbert, J., Daddi, E., Ellis, R.S., Elvis, M., Ewald, S.P., Fall, M., Franceschini, A., Giavalisco, M., Green, W., Griffiths, R.E., Guzzo, L., Hasinger, G., Impey, C., Kneib, J.P., Koda, J., Koekemoer, A., Lefevre, O., Lilly, S., Liu, C.T., McCracken, H.J., Massey, R., Mellier, Y., Miyazaki, S., Mobasher, B., Mould, J., Norman, C., Refregier, A., Renzini, A., Rhodes, J., Rich, M., Sanders, D.B., Schiminovich, D., Schinnerer, E., Scodreggio, M., Sheth, K., Shopbell, P.L., Taniguchi, Y., Tyson, N.D., Urry, C.M., Van Waerbeke, L., Vettolani, P., White, S.D.M., Yan, L., 2007a. COSMOS: Hubble Space Telescope Observations. *Astrophys. J. Suppl. Ser.* 172, 38–45. doi:10.1086/516580.

Scoville, N., Aussel, H., Brusa, M., Capak, P., Carollo, C.M., Elvis, M., Giavalisco, M., Guzzo, L., Hasinger, G., Impey, C., Kneib, J.P., LeFevre, O., Lilly, S.J., Mobasher, B., Renzini, A., Rich, R.M., Sanders, D.B., Schinnerer, E., Schiminovich, D., Shopbell, P., Taniguchi, Y., Tyson, N.D., 2007b. The Cosmic Evolution Survey (COSMOS): Overview. *Astrophys. J. Suppl. Ser.* 172, 1–8. doi:10.1086/516585.

Starck, J.L., Fadili, J., Murtagh, F., 2007. The undecimated wavelet decomposition and its reconstruction. *IEEE Transactions on Image Processing* 16, 297–309. doi:10.1109/TIP.2006.887733.

Starck, J.L., Murtagh, F., Fadili, J., 2015. doi:10.1017/CB09781316104514.

Vũ, B.C., 2013. A splitting algorithm for dual monotone inclusions involving cocoercive operators. *Advances in Computational Mathematics* 38, 667–681. URL: <https://doi.org/10.1007/s10444-011-9254-8>, doi:10.1007/s10444-011-9254-8.

Yuan, M., Lin, Y., 2006. Model selection and estimation in regression with grouped variables. *Journal of the Royal Statistical Society: Series B (Statistical Methodology)* 68, 49–67. doi:10.1111/j.1467-9868.2005.00532.x.

Zeng, X., Figueiredo, M.A., 2014. Decreasing weighted sorted ℓ_1 regularization. *IEEE Signal Processing Letters* 21, 1240–1244. doi:10.1109/LSP.2014.2331977.

Appendix A. Sparse2D Transforms

Appendix A.1. 1D Transforms

1. Linear wavelet transform: a trous algorithm
 2. B1spline wavelet transform: a trous algorithm
 3. B3spline wavelet transform: a trous algorithm
 4. Derivative of a b3spline: a trous algorithm
 5. Undecimated Haar wavelet transform: a trous algorithm
 6. Morphological median transform
 7. Undecimated (bi-) orthogonal wavelet transform
 8. Non orthogonal undecimated transform
 9. Modified positive B3spline wavelet transform: a trous algorithm
 10. Pyramidal b3spline wavelet transform
 11. Pyramidal median transform
 12. Morlet’s wavelet transform
 13. Mexican hat wavelet transform
 14. French hat wavelet transform
 15. Gaussian Derivative wavelet transform
 16. (bi-) orthogonal wavelet transform
 17. (bi-) orthogonal transform via lifting scheme
 18. Wavelet packets
 19. Wavelet packets from lifting scheme
 20. Wavelet packets using the a-trous algorithm)
 21. Pyramidal linear wavelet transform
- ### Appendix A.2. 2D and 2D1D Transforms
1. linear wavelet transform: a trous algorithm
 2. bspline wavelet transform: a trous algorithm
 3. wavelet transform in Fourier space
 4. morphological median transform
 5. morphological minmax transform
 6. pyramidal linear wavelet transform
 7. pyramidal bspline wavelet transform
 8. pyramidal wavelet transform in Fourier space: algo 1 (diff. between two resolutions)
 9. Meyer’s wavelets (compact support in Fourier space)
 10. pyramidal median transform (PMT)
 11. pyramidal laplacian
 12. morphological pyramidal minmax transform
 13. decomposition on scaling function
 14. Mallat’s wavelet transform (7/9 filters)
 15. Feauveau’s wavelet transform
 16. Feauveau’s wavelet transform without undersampling
 17. Line Column Wavelet Transform (1D+1D)
 18. Haar’s wavelet transform
 19. half-pyramidal transform
 20. mixed Half-pyramidal WT and Median method (WT-HPMT)
 21. undecimated diadic wavelet transform (two bands per scale)
 22. mixed WT and PMT method (WT-PMT)
 23. undecimated Haar transform: a trous algorithm (one band per scale)
 24. undecimated (bi-) orthogonal transform (three bands per scale)
 25. non orthogonal undecimated transform (three bands per scale)
 26. Isotropic and compact support wavelet in Fourier space
 27. pyramidal wavelet transform in Fourier space: algo 2 (diff. between the square of two resolutions)
 28. Fast Curvelet Transform
 29. Wavelet transform via lifting scheme
 30. 5/3 on line and 4/4 on column
 31. 4/4 on line and 5/3 on column
- ### Appendix A.3. 3D Transforms
1. (bi-) orthogonal transform
 2. (bi-) orthogonal transform via lifting scheme
 3. A trous wavelet transform

Appendix A.4. Curvelet Transforms

1. RectoPolar Ridgelet Transform using a standard bi-orthogonal WT
2. RectoPolar Ridgelet Transform using a FFT based Pyramidal WT
3. RectoPolar Ridgelet Transform using a Pyramidal WT in direct space
4. Finite ridgelet transform
5. Slant Stack Radon transform + FFT based pyramidal WT.
6. Slant Stack Radon transformand + bi-orthogonal WT
7. Slant Stack Radon transformand + pyramidal WT in direct space
8. Slant Stack Radon transformand + Undecimated Starlet WT